

See discussions, stats, and author profiles for this publication at: <https://www.researchgate.net/publication/277884777>

Product Distribution during Co-pyrolysis of Bituminous Coal and Lignocellulosic Biomass Major Components in a Drop-Tube Furnace

ARTICLE in ENERGY & FUELS · JUNE 2015

Impact Factor: 2.79 · DOI: 10.1021/acs.energyfuels.5b00374

CITATIONS

2

READS

25

5 AUTHORS, INCLUDING:



Zhiqiang Wu

Xi'an Jiaotong University

10 PUBLICATIONS 23 CITATIONS

SEE PROFILE



Shuzhong Wang

Xi'an Jiaotong University

75 PUBLICATIONS 656 CITATIONS

SEE PROFILE



Lin Chen

University of Newcastle

28 PUBLICATIONS 28 CITATIONS

SEE PROFILE



Haiyu Meng

Xi'an Jiaotong University

10 PUBLICATIONS 23 CITATIONS

SEE PROFILE

Product Distribution during Co-pyrolysis of Bituminous Coal and Lignocellulosic Biomass Major Components in a Drop-Tube Furnace

Zhiqiang Wu,^{†,‡} Shuzhong Wang,^{*,‡} Jun Zhao,[‡] Lin Chen,[‡] and Haiyu Meng[‡]

[†]School of Chemical Engineering and Technology, and [‡]Key Laboratory of Thermo-Fluid Science and Engineering, Ministry of Education, School of Energy and Power Engineering, Xi'an Jiaotong University, Xi'an, Shaanxi 710049, People's Republic of China

ABSTRACT: Co-pyrolysis of the coal blend with lignocellulosic biomass has a significant influence on final product composition of co-gasification and co-combustion. Successful evaluation of the product distribution during co-pyrolysis is very important to understand the overall co-thermochemical process. In this paper, product distribution, especially the gaseous product evolution during a kind of bituminous coal from northern of China blended with lignocellulosic biomass, major model components (cellulose, hemicellulose, and lignin) were explored in a drop-tube furnace from 600 to 1000 °C. The addition of three model components showed different synergistic effects in the product yields and gaseous product composition. Positive synergistic effects in the gas and tar yields were observed during co-pyrolysis of bituminous coal and cellulose, indicating that the addition of cellulose promoted the formation of volatile products. On the contrary, gas yields from co-pyrolysis of bituminous and lignin mixtures showed a negative synergetic effect. For bituminous and hemicellulose blends, a negative synergetic effect on the gas yield was found, except when the temperature was 600 °C. Whether a positive or negative synergistic effect existed in the composition depended upon the mixing ratio and temperature. Cellulose and hemicellulose showed a similar effect on the gas composition (H₂, CH₄, CO, and CO₂). The addition of cellulose and lignin promoted the proportion of CH₄ and light hydrocarbons (C₂H₄ and C₂H₆), respectively.

1. INTRODUCTION

Co-thermochemical conversion of lignocellulosic biomass and coal can provide a solution for use of biomass on a commercial scale and reduction of the carbon footprint and fossil fuel consumption.^{1–8} As the initial step for gasification and combustion, pyrolysis is a very important process that affects final product composition of the thermochemical process.^{9,10} Furthermore, pyrolysis is also a promising thermochemical technology, providing various chemicals and fuels, such as high-quality char and high-value gas and liquid products.^{2,11} The gas products have an advantage in compression and transportation and are applied widely in industries.³ Thus, investigation on the product distribution, especially gaseous products, from co-pyrolysis of coal and lignocellulosic biomass is very necessary to understand the co-thermochemical process.

Much attention has been on the yield and composition of the gaseous products from co-pyrolysis of different ranks of coals blended with various lignocellulosic biomass.^{9,12–14} Some investigators observed a synergistic effect on the formation of the gaseous products,^{3,4,6,8,10,15} while others reported the absence of the synergistic effect.^{12,16–19} Previous research on gaseous product evolution during co-pyrolysis is illustrated in Table 1. The synergistic effect on gaseous product evolution can be divided into four situations: synergy did not exist in both gas/volatile yield and composition; synergy did not exist in gas/volatile yield but in composition; synergy existed in gas/volatile yield but not in composition;^{8,20,21} and synergy existed in both gas/volatile yield and composition.^{21,22} Sadhukhan et al.¹⁶ found the absence of a synergistic effect in volatile from co-pyrolysis of wood and lignite. Moghtaderi et al. and Vuthaluru^{17,18} also found no synergy effect in co-pyrolysis of coal blended with radiata pine sawdust, wood waste, and wheat straw, respectively. Several researchers found a similar

phenomenon for the co-pyrolysis of gas product evolution.^{1,23,24} Sonobe et al.²¹ found that a synergistic effect existed in both pyrolysis gas yields and compositions during co-pyrolysis of lignite blended with corn cob; the proportion of CH₄ was 3 times more than that calculated on the basis of the weight of an individual sample at 400 °C. Yang et al.²² reported the same conclusion during co-pyrolysis of lignite and rice husk. Zhang et al.²⁵ reported that synergetic effects existed in the compositions of the gas from co-pyrolysis of legume straw with lignite. Furthermore, Aboyade et al.¹⁰ found that the gas yield during co-pyrolysis of coal and corn residues showed an additive manner, while a significant synergistic effect was found in the composition of the vapor phase.

The synergistic effect is as a result of various factors, such as the biomass species, intensity of the sample contact, reactor types, and experimental conditions.⁵ On the basis of the characteristics of the raw materials, the wide varieties and heterogeneity of the lignocellulosic biomass also influenced the synergistic effect.⁴ The main constituents of the lignocellulosic biomass are cellulose, hemicellulose, and lignin.^{9,26} The pyrolytic behavior of these constituents during co-pyrolysis provides insight into the interaction between coal and lignocellulosic biomass. The authors investigated the synergistic effect in the pyrolytic behavior and kinetic characteristic during co-pyrolysis of bituminous coal (BC) and three model compounds via a thermogravimetric analyzer (TGA) previously and found that the three model compounds did show different effects on the kinetic parameters and char yield under slow-

Received: February 17, 2015

Revised: May 30, 2015

Published: June 1, 2015

Table 1. Previous Research on the Gaseous/Volatile Products during Co-pyrolysis of Coal and Lignocellulosic Biomass^a

reference	reactor	samples	temperature/heating rate	gas analysis	synergy in gas/volatile yield	synergy in gas/volatile composition
Wang et al. ³⁴	FBR	lignite/corn cob	1000 °C/10 °C min ⁻¹	MS	yes	yes
Yang et al. ²²	VR	lignite/rice husk	900 °C/10 °C min ⁻¹	GC/TCD	yes	yes
Wang et al. ³⁵	FDBR	sub-bituminous/corn cob	700 °C	GC/TCD FID	no	yes
	TGA	sub-bituminous/corn cob	700 °C/10 and 40 °C min ⁻¹	none	yes	not mentioned
Song et al. ³⁶	TGA	lignite/pine sawdust	1000 °C/10 °C min ⁻¹	none	yes	not mentioned
	FBR	lignite/pine sawdust	400, 600, and 900 °C	GC/TCD	yes	yes
Quan et al. ³⁷	TGA	sub-bituminous/white pine	800 °C/10 °C min ⁻¹	none	yes	not mentioned
	DTF	sub-bituminous/white pine	600 °C	GC	yes	yes
Li et al. ³⁸	FBR	bituminous/rice straw	700, 800, and 900 °C	GC	yes	yes
Soncini et al. ⁹	DTF	sub-bituminous lignite/pine	975 °C/10 ³ °C min ⁻¹	MS	yes	yes
Rerkkaiwan et al. ²⁰	DTF	sub-bituminous/rice straw wood	800 °C	GC/TCD	yes	yes
Aboyade et al. ¹⁰	FBR	hard coal/sugar cane bagasse, corn residues	600 °C/10–15 °C min ⁻¹	GC/TCD	no	yes
Fermoso et al. ²⁴	FBR	bituminous/olive stones, chestnut	1000 °C/15 °C min ⁻¹	GC/TCD	no	no
Yuan et al. ³⁹	FBR	bituminous/rice straw	1200 °C/10 ³ °C min ⁻¹	GC	yes	yes
Park et al. ⁸	TGA	sub-bituminous/sawdust	900 °C/15 °C min ⁻¹	none	yes	not mentioned
	FBR	sub-bituminous/sawdust	800 °C	IR/TCD	yes	yes
Kajitani et al. ¹	DTF	bituminous/cedar bark	1400 °C	GC/TCD	no	no
Di Nola et al. ²³	TGA	woody/agricultural biomass	900 °C/10, 30, and 100 °C min ⁻¹	FTIR	no	no
Sonobe et al. ²¹	TGA	lignite/corn cob	600 °C/10 °C min ⁻¹	MS	no	no
	FBR	lignite/corn cob	300–600 °C/10 °C min ⁻¹	GC/TCD	yes	yes
Zhang et al. ²⁵	DTF	lignite/legume straw	500–700 °C	GC	yes	yes
Onay et al. ²	FBR	lignite/safflower seed	700 °C	none	yes	not mentioned
Jones et al. ⁴⁰	Py-GM	bituminous lignite/pine	900 °C	GC–MS	no	yes
Meesri et al. ¹²	FBR	Drayton coal/pine sawdust	400, 800, and 1000 °C/10 °C min ⁻¹	GC/TCD	no	no
	DTF	Drayton coal/pine sawdust	900 °C/10 ³ °C min ⁻¹	GC/TCD	no	no
Storm et al. ³¹	DTF	hard coal/straw	800 °C	GC/TCD FID	no	not mentioned
Collot et al. ¹⁹	FBR	Daw Mill/Polish coal/forest residue	850 and 1000 °C	none	no	not mentioned
	FDBR	Daw Mill/Polish coal/forest residue	850 and 1000 °C	none	no	not mentioned

^aFBR, fixed-bed reactor; VR, vacuum reactor; TGA, thermogravimetric analyzer; FDBR, fluidized-bed reactor; DTF, drop-tube furnace; Py-GM, pyrolysis–GC–MS; MS, mass spectrometer; GC, gas chromatography; TCD, thermal conductivity detector; FID, flame ionization detector; FTIR, Fourier transform infrared spectrometry; and IR, infrared gas analyzer.

pyrolysis conditions.⁴ However, there are few investigations on product distribution during pyrolysis of coal blends with lignocellulosic biomass major model compounds under fast heating conditions. The effect of the cellulose, hemicellulose, and lignin involved in this process have not yet been fully elucidated. To design the co-thermochemical process more efficiently and comprehensively on a large scale, there is an unmet need to explore the product distributions during pyrolysis of the coal blend with major biomass components.

The objective of this paper is to investigate the gaseous product evolution of lignocellulosic biomass model compounds and BC during co-pyrolysis to optimize the co-thermochemical conversion. Cellulose, hemicellulose, lignin, and BC mixtures were pyrolyzed in a drop-tube furnace (DTF) from 600 to 1000 °C. The influences of the mixing ratio and temperature on the product distribution were studied.

2. EXPERIMENTAL SECTION

2.1. Samples. The BC was collected from north of Shaanxi, China. Cellulose (CE, CAS Registry Number 9004-34-6), hemicellulose (HC, commonly representative by xylan from beechwood, CAS Registry Number 9014-63-5), and lignin (LG, alkali lignin, CAS Registry Number 8068-05-1) were purchased from Sigma–Aldrich Co., Ltd. The preparation of the raw samples and mixed samples were described in previous research.⁴ The mixtures of BC and CE were named as “BCCE1-1”, “BCCE1-2”, and “BCCE1-3”, which means that the mass ratio of CE was 25, 50, and 75%, respectively. The mixtures of BC and

HC and BC and LG were named the same way. The proximate and ultimate analysis information on the samples was illustrated in Table 2.

2.2. Methods. **2.2.1. Apparatus and Procedure.** The pyrolysis of BC, CE, HC, LG, and their mixtures was performed with a DTF (internal diameter of 35 mm and length of 800 mm), which was heated through an electric furnace. The sketch diagram of the DTF is shown in Figure 1. The experimental apparatus mainly consisted with the temperature and carrier gas control models, a DTF, and models for

Table 2. Proximate and Ultimate Analyses of the Raw Samples^a

	BC	CE	HC	LG
Proximate Analysis (wt %, ad)				
moisture, <i>M</i>	4.18	3.67	5.76	3.38
ash, <i>A</i>	15.38	0.07	3.61	3.62
volatile, <i>V</i>	30.56	94.37	77.71	60.35
fixed carbon, <i>FC</i>	49.88	1.89	12.92	32.65
Ultimate Analysis (wt %, daf)				
carbon, <i>C</i>	79.31	44.3	40.18	61.35
hydrogen, <i>H</i>	4.72	6.17	5.53	5.05
nitrogen, <i>N</i>	1.03		2.71	1.13
sulfur, <i>S</i> ^t	1.3	0.03		0.69
oxygen, <i>O</i> ^c	13.38	49.5	51.58	31.78
higher heating value (MJ kg ⁻¹ , ad)	25.44	16.71	15.21	17.98

^aad, air dried; daf, dry and ash free; t, total content; and c, calculated by difference.

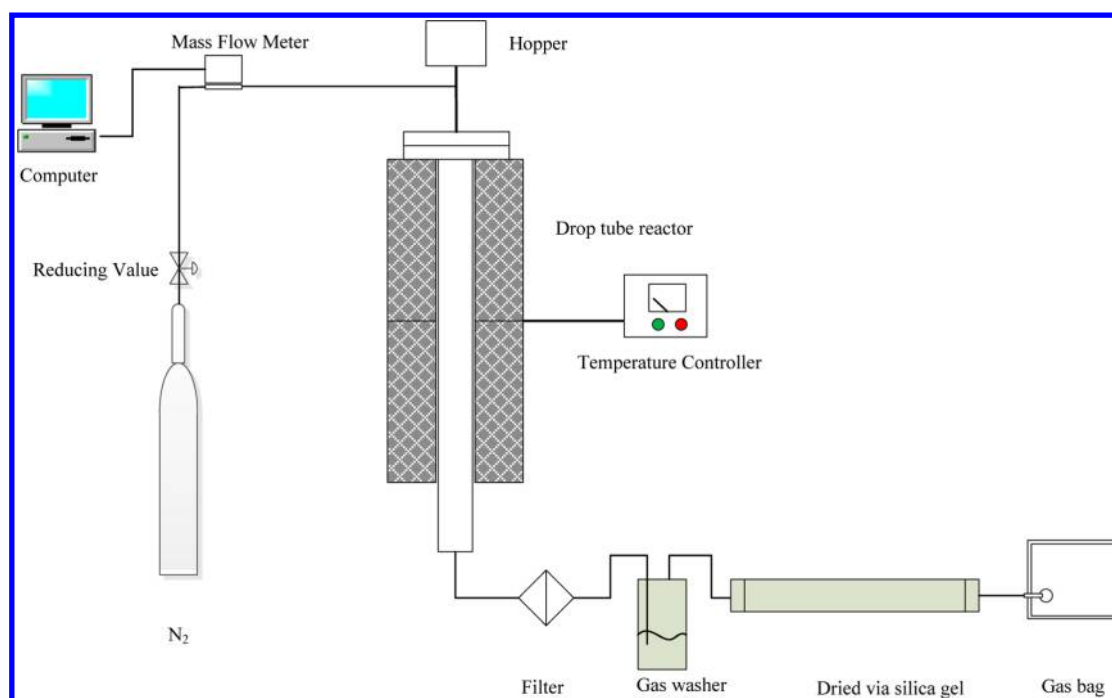


Figure 1. Schematic diagram of the DTF.

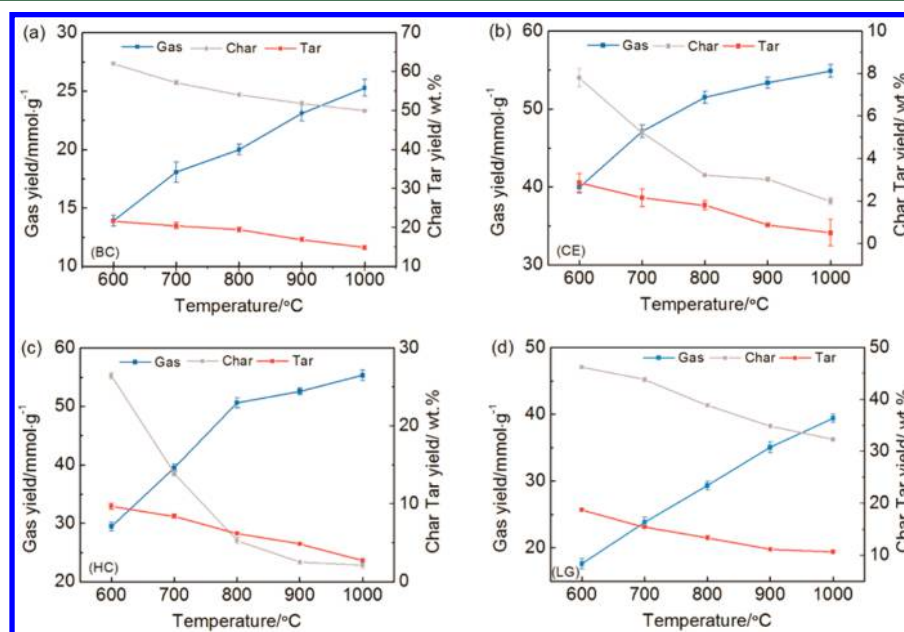


Figure 2. Product distribution of the BC and lignocellulosic biomass major components under different temperatures: (a) BC, (b) CE, (c) HC, and (d) LG.

purification, dehydration, and analysis. For each experiment, the DTF was heated from room temperature to the target temperature. The carrier gas was nitrogen, and it was maintained at a flow rate of 100 mL min⁻¹ during the heating and pyrolysis processes. The carrier gas was controlled by a mass flow meter. When the DTF reached the target temperature, it kept the target temperature constant for 10 min, and then the raw or mixed sample (1 g) was fed into the DTF. The gaseous products passed through a glass wool filter, followed by a gas washer, dried via silica gel, and then collected through a gas bag. The gathering time was 10 min from the sample drop into the reactor to make sure that the gas product was collected adequately for each sample. The yield of the gaseous product was calculated on the basis of the volume of the carrier gas. For each test, it was repeated 3 times to ensure the accuracy of the results.

2.2.2. Measurement of the Gaseous Products. The major constituents of the gas products (CO, CO₂, CH₄, C₂H₄, and C₂H₆) were quantitatively detected by BeiFen3420A gas chromatography with thermal conductivity detectors (TCDs). The Carboxen 1000 packed column was used with dimensions (60/80 mesh, 15 ft × 1/8 in. outer diameter). The furnace was programmed with an initial temperature of 40 °C to hold for 8.5 min, ramped at 50 °C min⁻¹ to 210 °C, and kept constant for 20 min. The temperature of the injector and detector was 80 and 100 °C, respectively. High-purity helium was the carrier gas with a flow rate of 30 mL min⁻¹. Quantification of each gaseous product was calculated on the basis of the response factors from a standard gas mixture.

In addition, the synergistic effect on the gaseous product yield and component during co-pyrolysis of BC and major model compounds

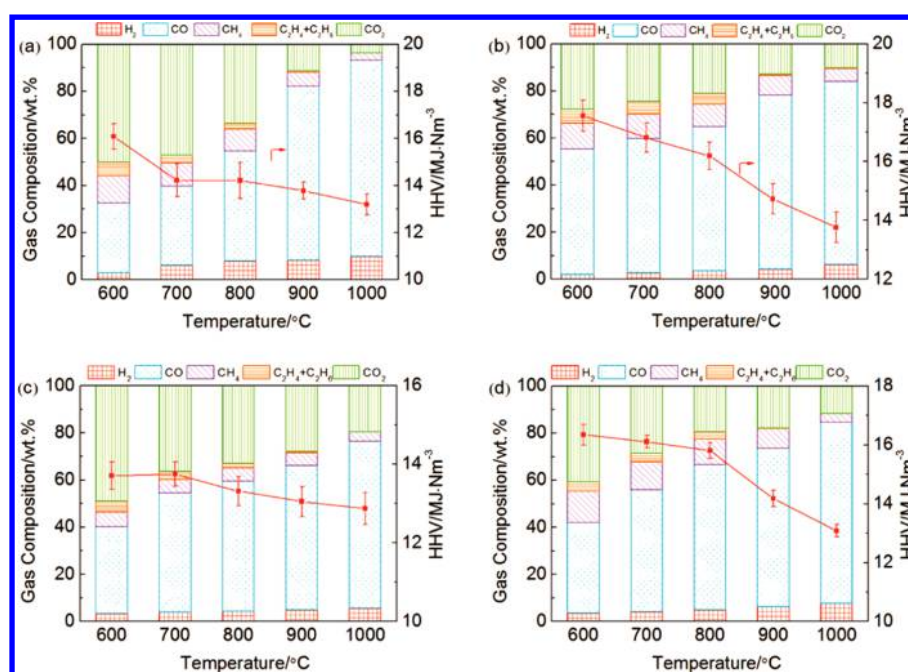


Figure 3. Gaseous product composition and heat value of the BC and lignocellulosic biomass major components: (a) BC, (b) CE, (c) HC, and (d) LG.

was evaluated from the difference of the experimental and predicted values. ΔW was defined to estimate the synergistic effect:

$$\Delta W = W_{\text{experiment}} - W_{\text{prediction}} \quad (1)$$

where ΔW is the relative deviation of the gas component (%) or yield (mmol g^{-1}), which represents the degree of the synergistic effects, $W_{\text{experiment}}$ is the experimental value for each gaseous product component (%) or gas yield (mmol g^{-1}), and $W_{\text{prediction}}$ is calculated on the basis of weight of the individual gaseous product component or gas yield of the contributing sample, which can be obtained by

$$W_{\text{prediction}} = X_C W_C + X_B W_B \quad (2)$$

where X_C and X_B are the mass ratio of the major model compounds (CE, HC, and LG) and BC in the mixtures and W_C and W_B are the gaseous product component or gas yield of major model compounds and BC under the same conditions of the mixture. For the effective components (H_2 , CO, CH_4 , C_2H_4 , and C_2H_6), when ΔW was greater than zero, a positive synergistic effect was observed during the copyrolysis process; When ΔW was less than zero, a negative synergistic effect was observed. For the CO_2 component in the gaseous products, the definition of a positive or negative synergistic effect was opposite those of the other effective components.

3. RESULTS AND DISCUSSION

3.1. Product Evolution of BC and Model Lignocellulosic Biomass Components. 3.1.1. Gas, Tar, and Char Yields of the Individual Samples.

The influence of the temperature on the product evolution is shown in Figure 2. For BC and lignocellulosic biomass major components, the yields of gas increased with an increasing pyrolysis temperature. The organic matter of CE was nearly totally released as the temperature increased to 1000 °C, which is consistent with previous work.²⁷

3.1.2. Gaseous Product Characteristics of the Individual Samples. The gas composition of BC and major model compounds from 600 to 1000 °C are shown in Figure 3. As shown in Figure 3, the major components of the gaseous products are mainly H_2 , CO, CH_4 , and CO_2 , along with light

hydrocarbons (C_2H_4 and C_2H_6). The yield of H_2 and CO for BC and major components increased with an increase in the temperature. On the contrary, CH_4 , CO_2 , and light hydrocarbons gradually decreased with the temperature increment, with light hydrocarbons even reducing to zero when the temperature reached 1000 °C. CO_2 was the key component of pyrolytic gaseous products of BC when the temperature was below 700 °C. While CO was the predominant component of pyrolytic products for CE and HC, which contributed more than 50% of the pyrolysis gas. As previously stated, the formation of CO_2 was from the decarboxylation reaction, accompanied with the thermal decomposition of oxygen-containing functional groups, such as carboxylic compounds.¹² It was also implied that the release of CO_2 during coal pyrolysis was related to cross-linking processes.²⁸ The cross-linking accompanied decomposition of carboxyl groups.^{28,29} Thus, the higher CO_2 content in the gaseous products for BC may be owed to the cross-linking process. The yield of CO_2 increase with the temperature may be due to the exothermic property of decarboxylation. A higher content of CO (from 53 to 77.85 wt %) was attributed to the enrichment of C–O compounds in the CE, which was consistent with other studies.²⁶ A higher heating value (HHV) of the pyrolysis gas was between 12 and 18 MJ Nm^{-3} , and the HHV was related to the composition of the gas. As the pyrolysis temperature increased, the HHV showed a decreasing tendency, which was due to the decrease of the light hydrocarbons with a high HHV. When the temperature increased, the rate of reforming reactions were promoted, resulting in a higher yield of hydrogen.³⁰ The change of CO and CO_2 was related to the Boudouard reaction ($\text{C} + \text{CO}_2 = 2\text{CO}$).³⁰ The decreasing of the light hydrocarbon (C_2H_4 and C_2H_6) yield with the increment of the temperature was due to the promotion of the cracking reactions. The yield of CO from BC was higher than that of H_2 , which was consistent with the previous research.³¹

3.2. Product Evolution of the Mixed Samples.

3.2.1. Gas, Tar, and Char Yields of the Mixed Samples. The

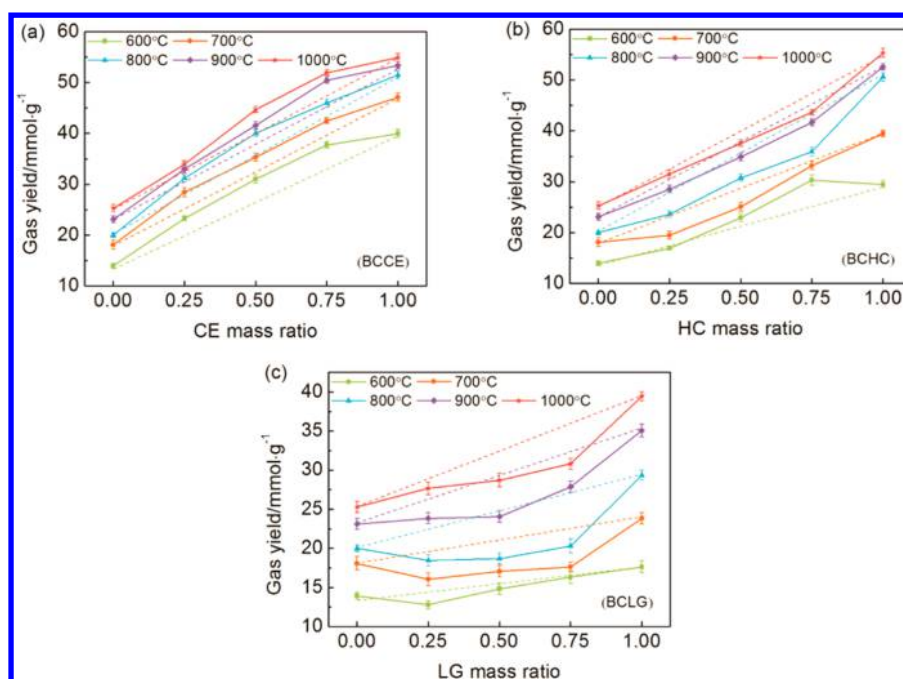


Figure 4. Experimental and predicted yields of gaseous products during co-pyrolysis of BC blended with lignocellulosic biomass major components: (a) bituminous coal and cellulose mixtures (BCCE), (b) bituminous coal and hemicellulose mixtures (BCHC), and (c) bituminous coal and lignin mixtures (BCLG) (dotted lines were the predicted gas yield calculated on the basis of the mass average of the BC and model compounds).

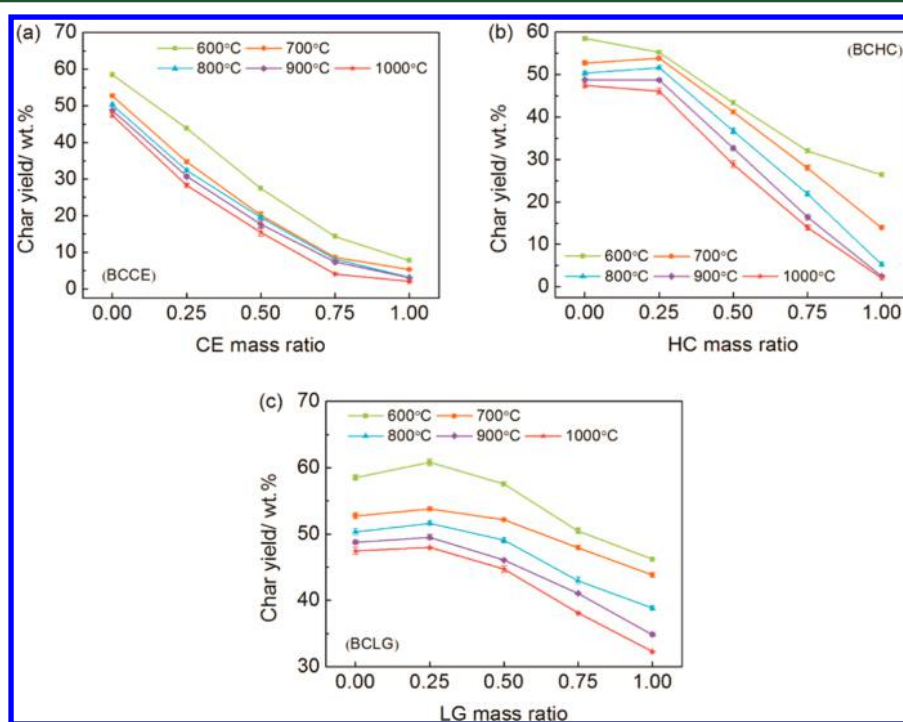


Figure 5. Char yields during co-pyrolysis of BC blended with lignocellulosic biomass major components: (a) bituminous coal and cellulose mixtures (BCCE), (b) bituminous coal and hemicellulose mixtures (BCHC), and (c) bituminous coal and lignin mixtures (BCLG).

experimental and predicted gas yields from co-pyrolysis of BC and the three major lignocellulosic biomass components from 600 to 1000 °C are shown in Figure 4. The solid lines represent gaseous products obtained from the experiment, and the dotted lines represent the prediction of the gas yield. It indicated that the gas yield of BC and three major components showed different gas yields, which was relevant to the variance in the molecular structure of the samples.²⁵ The gas yield of the BC,

HC, and LG was nearly 2, 1.5, and 1.2 times more than that of the BC at the same temperature, respectively. The primary structure of CE was a polysaccharide linked by β -1,4-glycosidic bonds, which were relatively weak linkages.⁴ The primary structure of HC was β -1,4-linked-D-mannose and D-glucose. While the molecular structure of BC was mainly linked by covalent bonds, which were more strongly bonded and resistive to the heat than that of the CE or other major components.

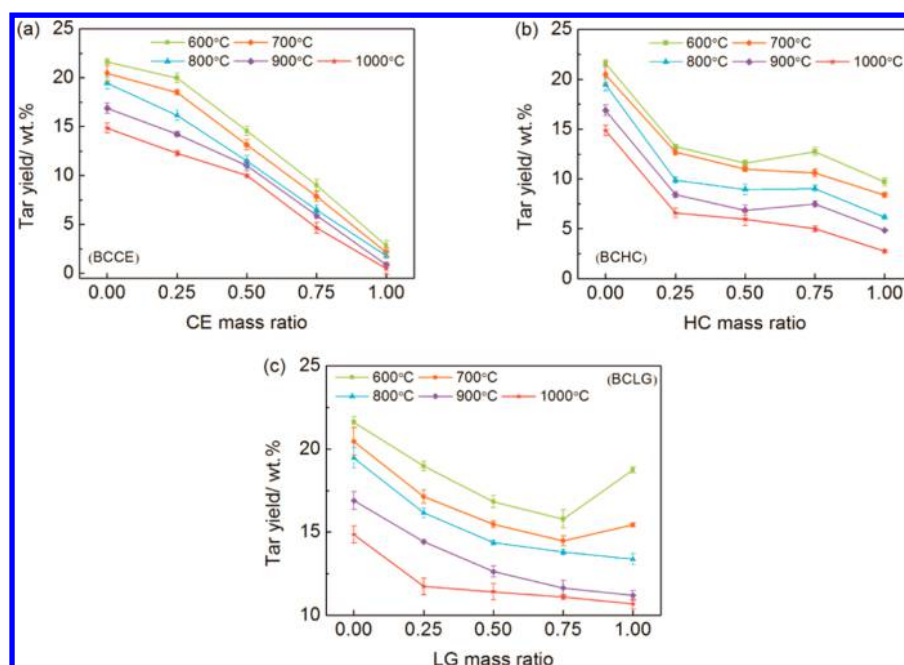


Figure 6. Tar yields during co-pyrolysis of BC blended with lignocellulosic biomass major components: (a) bituminous coal and cellulose mixtures (BCCE), (b) bituminous coal and hemicellulose mixtures (BCHC), and (c) bituminous coal and lignin mixtures (BCLG).

Thus, the gas yields of the major components were higher than that of the BC.

Furthermore, for BC and CE mixtures, the gas yield was increased with the CE mass ratio from 600 to 1000 °C. The predicted gaseous product yields were less than those of experimental values, deviating most at 600 °C. This can be due to the higher H/C and O/C molar ratios of CE, which were about 2.33 and 6.59 times more than those of BC. Thus, during thermal decomposition of CE, a lot of H and OH radicals were generated with the breakdown of glycosidic bonds. Those hydrogenous donors promoted the cracking of aromatic structures in the BC.²⁰ The addition of CE restrains the secondary reactions, including cross-linking condensation and repolymerization reactions, resulting in less char and tar formation.⁸

Figure 4b shows the effects of HC on the gas yield of the mixture; the gas yield was increased with the HC mass ratio increasing. The experimental gas yields of the BCHC were higher than the calculated values at 600 °C, indicating that the addition of HC promoted the decomposition of the BC. A positive synergy effect was observed in the gas yield. However, when the temperature increased to 700 °C and above, the gas formation was suppressed, and a negative synergetic effect in the gas yield was observed. The changing of the synergetic effect agreed with the reported co-pyrolysis of BC and HC in a TGA.⁴ Figure 4c illustrated the effect of LG on the gas yields from co-pyrolysis of BC and LG. As the temperature increased from 600 to 800 °C, the gas yields of the BCLG first decreased at 25% LG mass ratio and then increased gradually with the increasing of the LG mass ratio. When the pyrolysis temperatures were 900 and 1000 °C, the tendency of the gas yield was similar to those of BCCE and BCHC. In contrast with the synergistic effect in the gas yield between BC and CE, the experimental gas yield obtained from BCLG was lower than that calculated on the basis of the mass average of the BC and LG. A negative synergistic effect was found on the gas yield during co-pyrolysis of BC blended with LG.

The char and yields of the BC and three model compound mixtures from 600 to 1000 °C are shown in Figures 5 and 6, respectively. For BCCE mixtures, both the char and tar yields decreased with the CE mass ratio. The experimental char yield of BCCE was lower than that calculated on the basis of the mass average of the BC and CE, indicating that a negative synergistic effect was found in the char yield, while a positive synergistic effect was observed in the tar yield because of the higher volatile content in CE.^{4,26} In contrast, the variation of char yields for BCHC and HCLG showed a similar tendency. The calculated char yields of BCHC and BCLG were higher than the experimental values, which means a positive synergistic effect in the char yield during co-pyrolysis of BC and HC and BC and LG. As the temperature was raised, the tar yield declined because of the strengthening on cracking and reforming of the primary and secondary tar compounds.

3.2.2. Gaseous Product Characteristics of BC and CE Mixtures. The gaseous product characteristics of BC blended with CE are illustrated in Figure 5. From Figure 7a, it can be seen that the composition of H₂ initially increased with the CE mass ratio of 25% and, afterward, decreased gradually with the increase in the ratio of CE at 600 °C. As the temperature increased above 700 °C, the addition of CE reduced the yield of H₂ and the minimum value was obtained under 50% CE mass ratio. This indicated that the release of H₂ was promoted mainly in a lower temperature and CE mass ratio, while a higher temperature and CE mass ratio may inhibit the formation of H₂. The formation of H₂ from CE is mainly from the secondary tar cracking reaction.

Panels b and c of Figure 7 illustrated the variation of CO and CO₂ composition with the CE mass ratio and temperature. CO and CO₂ formed from decarbonylation and decarboxylation reactions. When the pyrolysis temperature was raised from 600 to 800 °C, the CO yield increased with the CE mass ratio. At 75% CE mass ratio and 800 °C, the composition of CO was greater than 65 wt %, indicating that the release of CO was accelerated as the temperature and CE mass ratio increased.

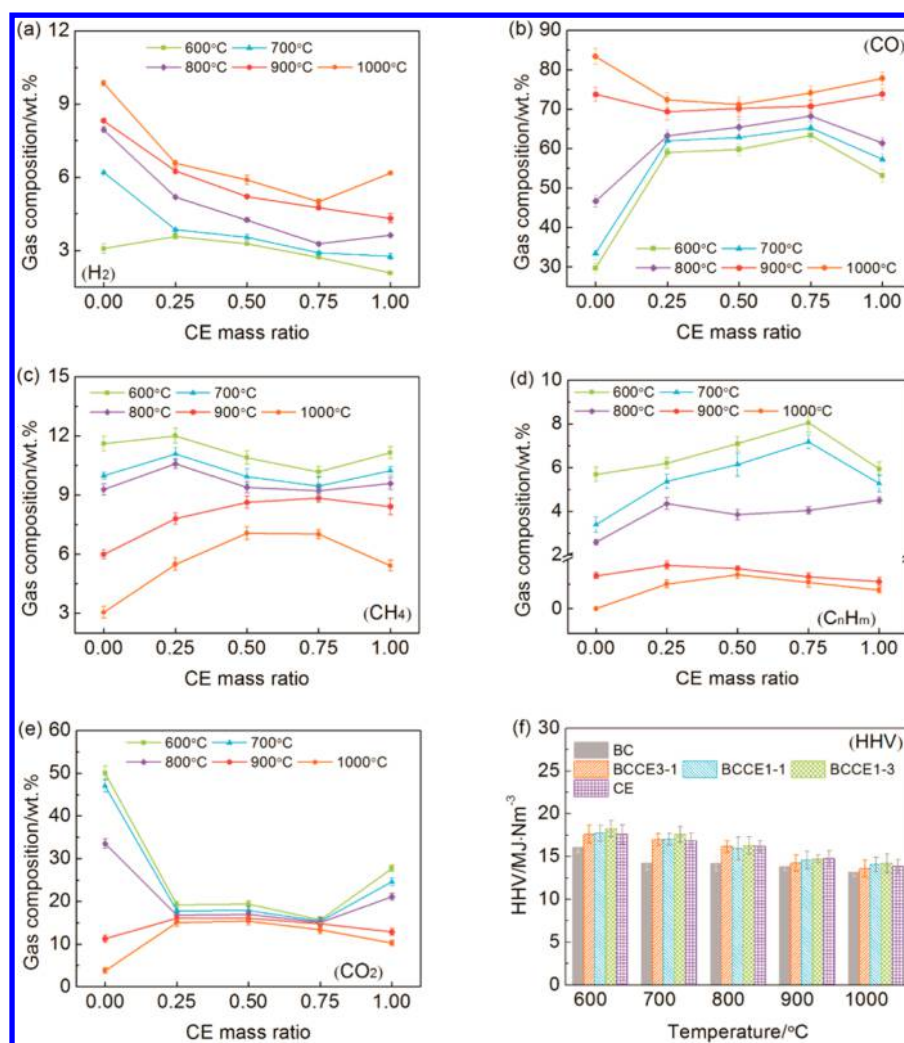


Figure 7. Effect of CE on the composition and heat value of the co-pyrolysis of gaseous products: (a) H_2 , (b) CO , (c) CH_4 , (d) C_2H_4 and C_2H_6 , (e) CO_2 , and (f) HHV.

For CO_2 , the tendency was opposite that of CO . CO_2 was also implied from the rapid secondary process during char formation. The distribution characteristics of CH_4 and other light hydrocarbons (C_2H_4 and C_2H_6) are shown in panels d and e of Figure 7. All of them decreased with the increase in the temperature and the same CE mass ratio. The composition of CH_4 increased with the CE mass ratio increasing at 900 and 1000 °C, which was similar to that of CO_2 at the same temperature. From the results discussed above, the addition of CE had a different influence on the gaseous pyrolytic products of BC. The variation of H_2 , CO , CO_2 , CH_4 , C_2H_4 , and C_2H_6 suggested that an interaction existed between BC and CE, and the interaction cannot be ignored.

3.2.3. Gaseous Product Characteristics of BC and HC Mixtures. Figure 8 shows the influence of HC on the composition of each gaseous component. The main gas products from co-pyrolysis of BC and HC were CO and CO_2 . Figure 8a illustrates the variation of H_2 components with the HC mass ratio at different temperatures, which was similar to the tendency of BCCE. When the temperature was 600 °C, the H_2 proportion first increased from 3.0 to 4.45%, then slightly declined to 4.0% at 50% HC mass ratio, and rose to 4.18% at 75% HC mass ratio. When the temperature was greater than or equal to 700 °C, the H_2 content decreased with

the increment of the HC mass ratio. The effect of HC on the CO content in the co-pyrolysis gas is shown in Figure 8b. The proportion of the CO component increased with the HC mass ratio as the temperature increased from 900 to 1000 °C. However, as the temperature increased to 900 and 1000 °C, the tendency was in contrast with the lower temperature conditions. The formation of CO from HC was mainly from dehydrogenation of hydroxyls and cracking of carbonyl groups.²⁶ CO from pyrolysis of BC originated mainly from the cracking of ether bonds and phenolic hydroxyls.¹¹ When the temperature was less than 900 °C, the addition of HC promoted both dehydrogenation reactions and oxygen-containing group decomposition. Composition of CH_4 increased with the HC mass ratio increasing as the temperature was raised from 600 to 800 °C. When the temperature was 900 and 1000 °C, the CH_4 proportion first increased and subsequently declined. During pyrolysis of HC, CH_4 was mainly from the cracking of methoxy fractures and volatile products, while for BC, at a low temperature, CH_4 generated from decomposition of straight chains and branch chains and, at a high temperature, CH_4 was mainly from cracking of aromatic rings.¹¹ At a higher temperature (900 and 1000 °C) and lower HC mass ratio (25%), the addition of HC promoted

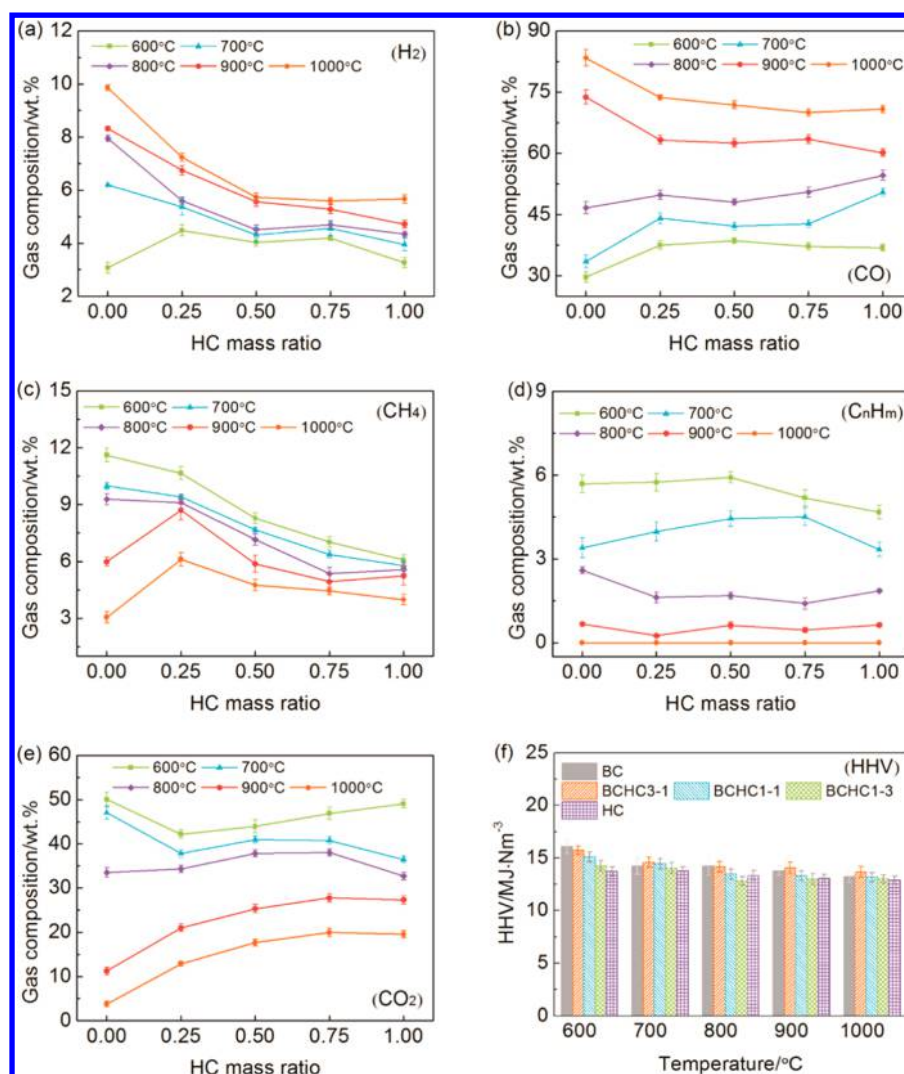


Figure 8. Effect of HC on the composition and heat value of the co-pyrolysis gaseous products: (a) H_2 , (b) CO , (c) CH_4 , (d) C_2H_4 and C_2H_6 , (e) CO_2 , and (f) HHV.

cracking of aromatic rings in BC. The distribution of light hydrocarbon components was similar to CH_4 .

The distribution of the CO_2 content is shown in Figure 8e; the content of CO_2 decreased first and then increased when the temperature was 600 and 700 °C. When the temperature was between 800 and 1000 °C, the CO_2 proportion increased with the HC mass ratio. During the pyrolysis of HC, CO_2 mainly generated from reforming reactions of carboxyl and carboxylic acid.²⁶ During the pyrolysis of BC, CO_2 was mainly from decomposition of the oxygen-containing groups. Under a higher temperature, the addition of HC promoted the formation of CO_2 . The HHV of the pyrolysis gas is shown in Figure 8f; the HHV of the BCHC was lower than that of BC generally and was in the range of 12.81–115.74 MJ Nm^{-3} .

3.2.4. Gaseous Product Characteristics of BC and LG Mixtures. The influence of LG on the composition of the gaseous component is shown in Figure 9. The main gas products during co-pyrolysis of BC and LG were similar to those of BCCE and BCHC, which were mainly CO and CO_2 (77.25–86.11%). With the increment of the temperature, the proportion of H_2 and CO increased and the proportion of CO_2 , CH_4 , and light hydrocarbons decreased. As shown in Figure 9a, the composition of H_2 increased from 3.00 to 4.93% and then

gradually decreased to 4.48, 4.31, and 3.51% under 600 °C, respectively. As the temperature increased, the addition of LG inhibited the formation of H_2 . The variation of H_2 at 1000 °C shows the reverse trend to 600 °C; it decreased from 10.0 to 8.0%. Figure 9b shows the content of CO derived from BC and LG. As the LG increased, the percentage of CO increased when the temperature was between 600 and 800 °C, and the increase of CO was more remarkable at 800 °C. Moreover, as the pyrolysis temperature increased to 900 and 1000 °C, CO composition decreased with the increase of the LG mass ratio. The tendency of CO_2 composition was in contrast with that of CO , as seen in Figure 9e. During the pyrolysis of LG, CO and CO_2 were mainly from the breaking and reforming of carbonyl, carboxyl, and ether bonds on the side chain of benzene and also from the secondary cracking of volatile. For BC, CO and CO_2 were from cracking of oxygen-containing groups. During co-pyrolysis of BC and LG, there was competition between the formation of CO and CO_2 . When the temperature was between 600 and 800 °C, the formation of CO was dominant. When the temperature was 900 and 1000 °C, the formation of CO_2 was dominant.

The contents of CH_4 and light hydrocarbon gas product were illustrated in panels c and d of Figure 9. The composition

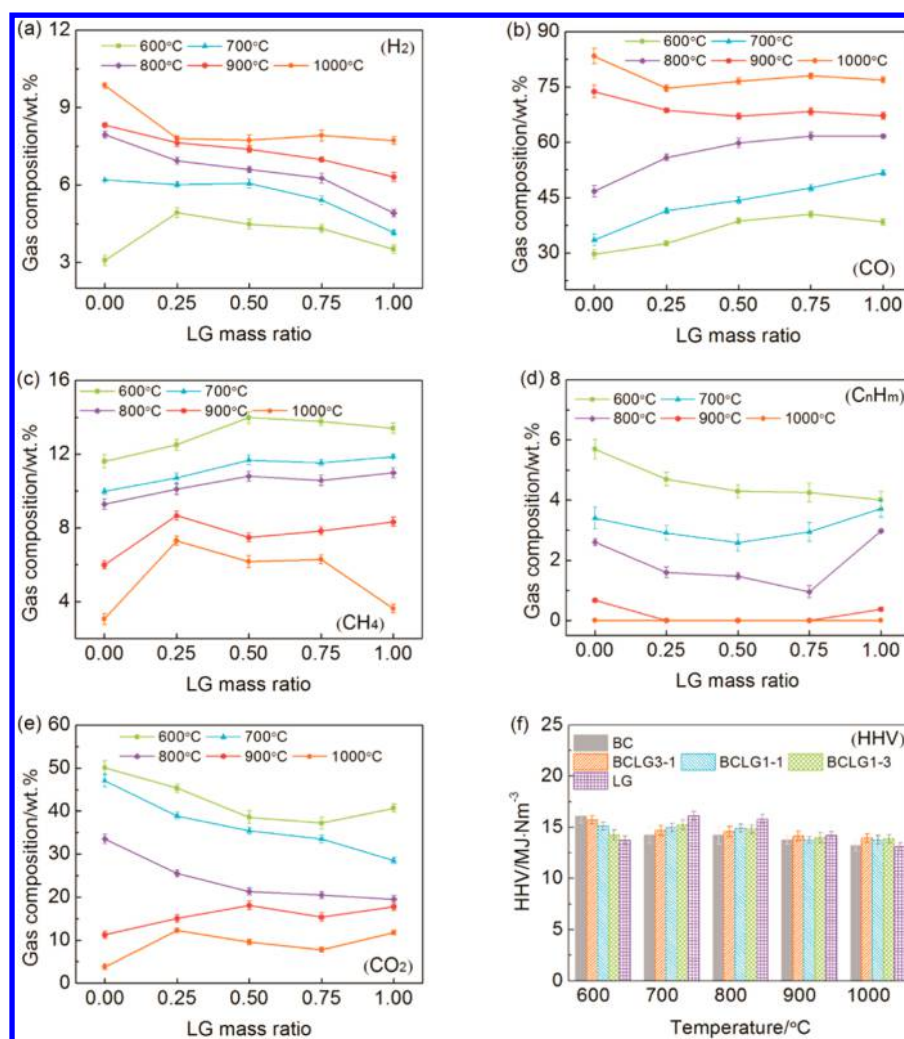


Figure 9. Effect of LG on the composition and heat value of the co-pyrolysis gaseous products: (a) H_2 , (b) CO , (c) CH_4 , (d) C_2H_4 and C_2H_6 , (e) CO_2 , and (f) HHV.

of CH_4 first increased and then decreased when the temperature was 600 and 700 °C. When the temperature was raised from 800 to 1000 °C, the CH_4 proportion increased with the LG mass ratio. During the pyrolysis of LG, CH_4 was mainly from the cracking of the side chain of phenylpropane, and as the temperature increased, the demethylation reaction of methoxyl functional groups resulted in the generation of CH_4 .³² The HHV was less than those of BCCE and BCHC, in the range of 13.76–16.43 MJ Nm^{-3} .

3.3. Synergistic Effects on Characteristics of Gaseous Products. 3.3.1. Synergistic Effects between the BC and CE.

The comparison of gaseous product composition from mixed samples to that calculated from the weighted average of individual BC and CE under the same conditions is shown in Figure 10. Figure 10a presents the variation trends of the H_2 composition from 600 to 1000 °C. The experimental values of H_2 under three mass ratios were higher than the predicted values at 600 °C. With the temperature increased, the deviation became less than zero, which indicated that the formation of H_2 was hindered with the addition of CE at a higher temperature.

The variations of CO composition between experimental and prediction values are shown in Figure 10b. It can be seen that the value of $W_{\text{experiment}}$ was higher than that of $W_{\text{prediction}}$ when the temperature was less than 800 °C, indicating that a positive

synergistic effect on CO composition between BC and CE did exist. This synergistic effect promoted the release of CO when the temperature was less than 800 °C, which can be named as a positive synergistic effect. While the temperature was higher than 900 °C, the variation trends were opposite the previous, which can be named as a passive synergistic effect on the formation of CO . It is illustrated from Figure 10c that the deviation curves of the $W_{\text{experiment}}$ and $W_{\text{prediction}}$ values for CO_2 of the mixed samples showed an opposite tendency to those of CO .

It can be observed from Figure 10d that, when the CE mass ratio was 25%, $W_{\text{experiment}}$ was always larger than $W_{\text{prediction}}$ when the temperature was raised from 600 to 1000 °C, which meant that the formation of CH_4 was accelerated. For 50 and 75% CE mass ratios, the same tendency was found when the temperature was higher than 800 °C. For composition of C_2H_4 and C_2H_6 , $W_{\text{experiment}}$ was higher than $W_{\text{prediction}}$ at the whole temperature range. This meant that positive synergistic effects on light hydrocarbons may exist during co-pyrolysis of BC and CE.

3.3.2. Synergistic Effects between the BC and HC. The difference in values between the experimental and predicted compositions of the gaseous products from co-pyrolysis of BC and HC is shown in Figure 11. The experimental value of H_2

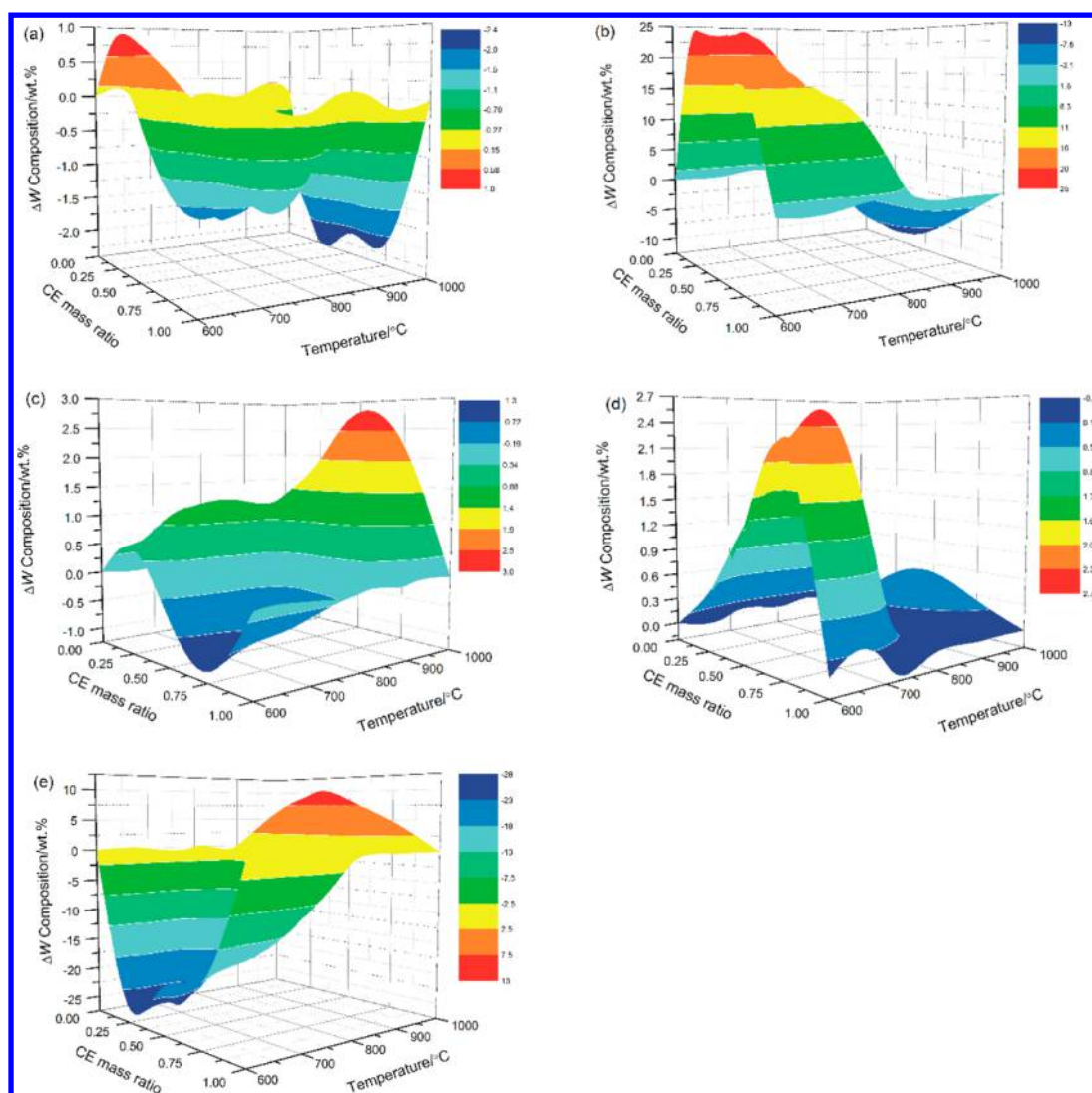


Figure 10. Comparison between the experimental and predicted major gas composition from the values during co-pyrolysis of BC and CE: (a) H_2 , (b) CO , (c) CH_4 , (d) C_2H_4 and C_2H_6 , and (e) CO_2 .

composition was higher than the predicted value when the pyrolysis temperature was 600 °C. However, as the temperature increased to greater than or equal to 700 °C, the content of H_2 was lower than the predicted value. The addition of HC in a higher temperature prevented the cracking of the aromatic rings in the BC.¹¹ The difference of CO components between the experimental and predicted values is shown in Figure 11b. When the temperature was between 600 and 800 °C and the HC mass ratio was 25%, the ΔW of CO composition was larger than zero, indicating that the formation of CO was promoted during co-pyrolysis of BC and HC. Nevertheless, with the increase in the HC mass ratio, the value of ΔW became less than zero at the temperature of 700 °C. During co-pyrolysis of BC and HC, CO was mainly from the decarbonylation and deacidification of HC and cracking of oxygen-containing functional groups of BC, respectively. At a higher HC mixing ratio and temperature, the decarbonylation reaction was inhibited, with the reduction of CO .³³ The tendency of CO_2 was opposite that of CO , which can be observed from Figure 9e. When the temperature was higher than 800 °C, the experimental value of the CO_2 content was higher than that of the calculated value based on an individual sample. The

addition of HC promoted the decarboxylic reaction during co-pyrolysis; thus, more CO_2 was generated.⁸ The addition of 25% HC promoted CH_4 formation when the temperature was between 600 and 900 °C. As the HC mass ratio increased, the experimental value of the CH_4 content was less than the predicted value when the temperature was less than 900 °C, indicating that the decomposition of straight chains and branch chains in BC was blocked.²³ The difference of light hydrocarbon gas-phase products expressed an opposite tendency to that of CH_4 . During pyrolysis of HC, the decomposition of unstable initial pyrolysis products and depolymerization of the aromatic structures generated CH_4 and light hydrocarbon gas.³³ During the co-pyrolysis of BC and HC, the formation of CH_4 and light hydrocarbon gas competed with each other, and a lower temperature and HC mass ratio were beneficial to the formation of C_2H_4 and C_2H_6 .

3.3.3. Synergistic Effects between the BC and LG. The deviations between experimental and predicted compositions of the gaseous products during co-pyrolysis of BC and LG are illustrated in Figure 12. When the temperature and LG mass ratio were less than 900 °C and 50%, the experimental value of the H_2 content was higher than the calculated, indicated

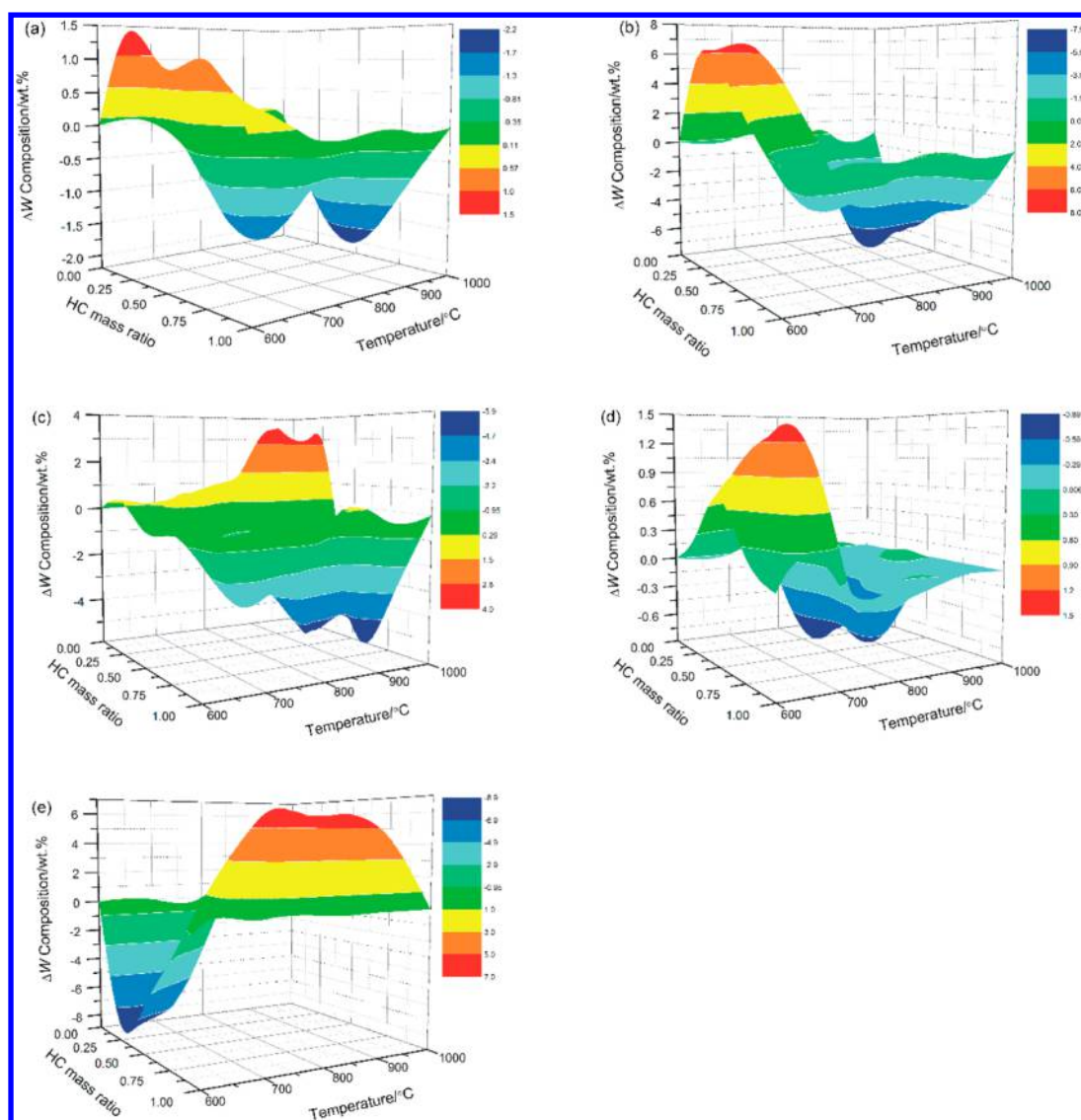


Figure 11. Comparison between the experimental and predicted major gas composition from the values during co-pyrolysis of BC and HC: (a) H_2 , (b) CO , (c) CH_4 , (d) C_2H_4 and C_2H_6 , and (e) CO_2 .

positive synergistic effect that existed during co-pyrolysis of BC and LG. During pyrolysis of LG, H_2 was mainly from depolymerization of the phenyl groups.⁸ In comparison to CE and HC, LG promoted the proportion of H_2 under a higher temperature and LG mass ratio. A positive synergistic effect on the CO content was found when the temperature was less than $900\text{ }^\circ\text{C}$. The synergistic effect on the CH_4 content during co-pyrolysis of BCLG was different from BCCE and BCHC. The predicted value of CH_4 was less than the experimental results in the experimental conditions of this paper, indicating that the addition of LG enhanced the decomposition of methoxy groups during the co-pyrolysis process.³³

As stated above, there is still some debate about whether there exist synergistic effects on the gas/volatile yields during co-pyrolysis of coal and lignocellulosic biomass. In this paper, synergy was found in the gas yields during co-pyrolysis of BC and three major model components. BC, HC, and LG had different effects on the co-pyrolysis process. Positive and negative synergistic effects on the yields of gaseous products were observed during co-pyrolysis of BCCE and BCLG from 600 to $1000\text{ }^\circ\text{C}$, respectively. For BCHC, the pyrolysis

temperature had a significant effect on the synergy. It has been reported that the gas yield obtained from the experiment was higher than that of the calculated value during co-pyrolysis of coal and biomass. Some researchers reported that the optimum condition for lignite/legume straw and sub-bituminous/sawdust mixture was $600\text{ }^\circ\text{C}$, where plenty of hydrogen donors and free radical were generated.^{8,25} Furthermore, the optimum condition for gas production was probably due to the positive synergistic effects of the BC and HC at $600\text{ }^\circ\text{C}$. The competition of the three main compounds on the gas generation may be the explanation about the conflicting results on the synergistic effect of gas yields.

Synergetic effects on the composition of gaseous products were observed during co-pyrolysis of BC blended with three major model compounds in a DTF. Significant deviations were observed between the experiment and predication values of major gaseous products, which will be beneficial to adjust and control the co-thermochemical process to gain high-value products. These results could give necessary information for understanding the interaction between lignocellulosic biomass and coal. A further study will focus on the effects of major

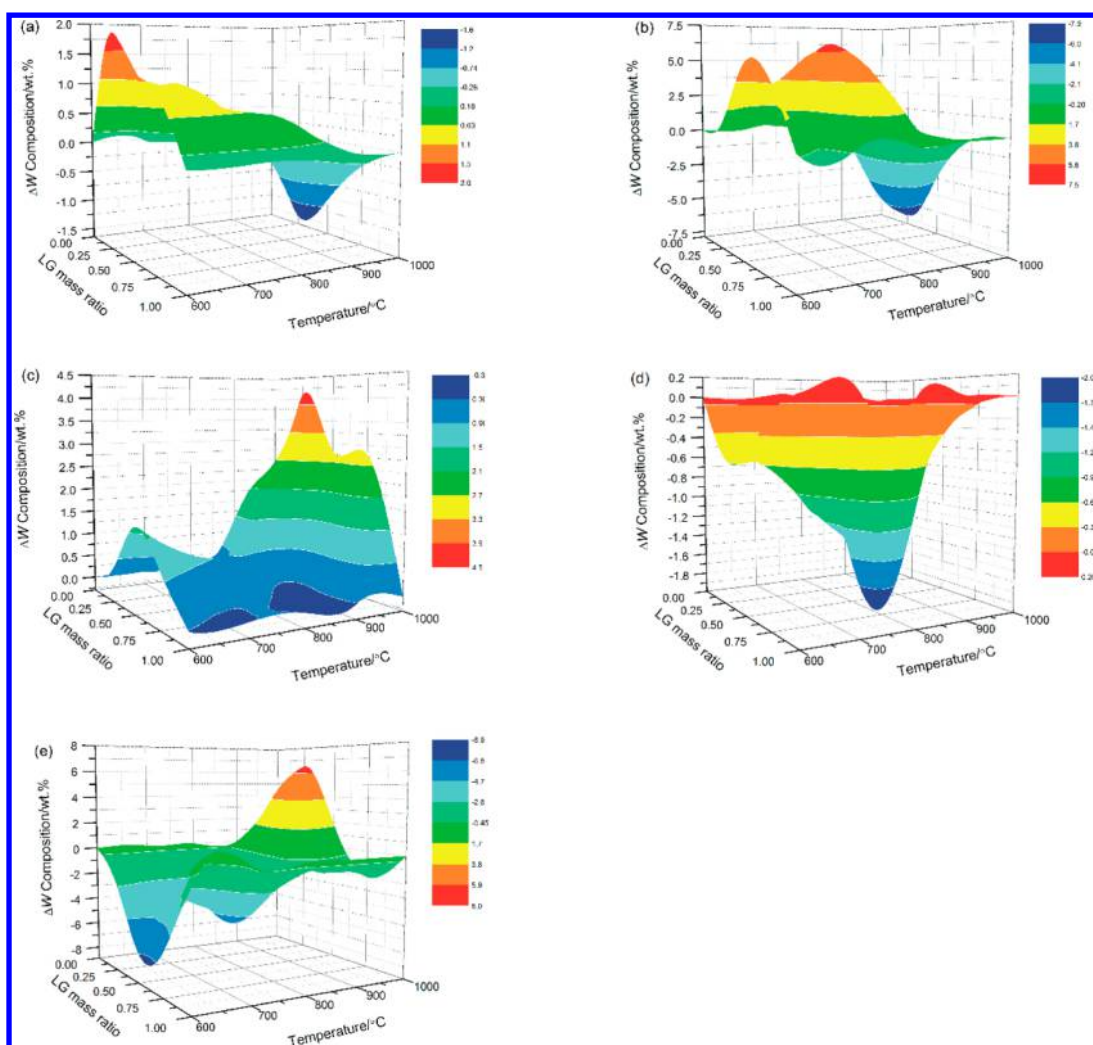


Figure 12. Comparison between the experimental and predicted major gas composition from the values during co-pyrolysis of BC and LG: (a) H_2 , (b) CO , (c) CH_4 , (d) C_2H_4 and C_2H_6 , and (e) CO_2 .

compounds on the evolution of char and tar during co-pyrolysis with coal.

4. CONCLUSION

The evolution of gaseous products from fast pyrolysis of coal, cellulose, hemicellulose, lignin, and their blends was investigated in a DTF. Synergistic effects on gaseous products yields and composition during co-pyrolysis of BC and major components were observed. The addition of cellulose promoted the yield of gaseous products, with a positive synergistic effect, while lignin inhibited the formation of gas during co-pyrolysis, indicating that a negative synergistic effect on the gas yield was observed. For coal and hemicellulose, a positive or negative synergistic effect on the gas yield was related to the temperature. A positive or negative synergistic effect on the composition of gaseous products depended upon the mixing ratio of the major compounds and pyrolysis temperature. The synergistic effects on the evolution of gaseous products from co-pyrolysis of coal and lignocellulosic biomass would be attributed to the competition between major model compounds.

AUTHOR INFORMATION

Corresponding Author

*Telephone: +86-29-82665157. Fax: +86-29-82668708. E-mail: szwang@aliyun.com.

Notes

The authors declare no competing financial interest.

ACKNOWLEDGMENTS

This work was financially supported by the Low-Carbon Development Special Fund of Guangdong Province, China (2011-1273). The authors are thankful to Professor BoLun Yang from the School of Chemical Engineering and Technology in Xi'an Jiaotong University for his constructive suggestions. The authors are thankful to Zhihui Wu and Caijian Zeng from the Guangdong Xi'an Jiaotong University Academy for their support of this work. Zhiqiang Wu is also grateful to Dongxia Ouyang from the ZhongTai Specialty Financing for her valuable suggestions.

REFERENCES

- (1) Kajitani, S.; Zhang, Y.; Umemoto, S.; Ashizawa, M.; Hara, S. Co-gasification reactivity of coal and woody biomass in high-temperature gasification. *Energy Fuels* **2010**, *24*, 145–151.

- (2) Onay, O.; Bayram, E.; Kockar, O. M. Copyrolysis of Seyitömer–lignite and safflower seed: Influence of the blending ratio and pyrolysis temperature on product yields and oil characterization. *Energy Fuels* **2007**, *21* (5), 3049–3056.
- (3) Wu, Z. Q.; Wang, S. Z.; Zhao, J.; Chen, L.; Meng, H. Y. Thermal behavior and char structure evolution of bituminous coal blends with edible fungi residue during co-pyrolysis. *Energy Fuels* **2014**, *28* (3), 1792–1801.
- (4) Wu, Z. Q.; Wang, S. Z.; Zhao, J.; Chen, L.; Meng, H. Y. Synergistic effect on thermal behavior during co-pyrolysis of lignocellulosic biomass model components blend with bituminous coal. *Bioresour. Technol.* **2014**, *169*, 220–228.
- (5) Shi, X.; Wang, J. A comparative investigation into the formation behaviors of char, liquids and gases during pyrolysis of pinewood and lignocellulosic components. *Bioresour. Technol.* **2014**, *170*, 262–269.
- (6) Chen, C.; Ma, X.; He, Y. Co-pyrolysis characteristics of microalgae *Chlorella vulgaris* and coal through TGA. *Bioresour. Technol.* **2012**, *117*, 264–273.
- (7) Vamvuka, D.; Sfakiotakis, S. Combustion behaviour of biomass fuels and their blends with lignite. *Thermochim. Acta* **2011**, *526* (1–2), 192–199.
- (8) Park, D. K.; Kim, S. D.; Lee, S. H.; Lee, J. G. Co-pyrolysis characteristics of sawdust and coal blend in TGA and a fixed bed reactor. *Bioresour. Technol.* **2010**, *101* (15), 6151–6156.
- (9) Soncini, R. M.; Means, N. C.; Weiland, N. T. Co-pyrolysis of low rank coals and biomass: Product distributions. *Fuel* **2013**, *112*, 74–82.
- (10) Aboyade, A. O.; Carrier, M.; Meyer, E. L.; Knoetze, H.; Gorgens, J. F. Slow and pressurized co-pyrolysis of coal and agricultural residues. *Energy Convers. Manage.* **2013**, *65*, 198–207.
- (11) Xu, Y. L.; Chen, B. L. Investigation of thermodynamic parameters in the pyrolysis conversion of biomass and manure to biochars using thermogravimetric analysis. *Bioresour. Technol.* **2013**, *146*, 485–493.
- (12) Meesri, C.; Moghtaderi, B. Lack of synergetic effects in the pyrolytic characteristics of woody biomass/coal blends under low and high heating rate regimes. *Biomass Bioenergy* **2002**, *23* (1), 55–66.
- (13) Aboyade, A. O.; Gorgens, J. F.; Carrier, M.; Meyer, E. L.; Knoetze, J. H. Thermogravimetric study of the pyrolysis characteristics and kinetics of coal blends with corn and sugarcane residues. *Fuel Process. Technol.* **2013**, *106*, 310–320.
- (14) Pan, Y. G.; Velo, E.; Puigjaner, L. Pyrolysis of blends of biomass with poor coals. *Fuel* **1996**, *75* (4), 412–418.
- (15) Weiland, N. T.; Means, N. C.; Morreale, B. D. Product distributions from isothermal co-pyrolysis of coal and biomass. *Fuel* **2012**, *94* (1), 563–570.
- (16) Sadhukhan, A. K.; Gupta, P.; Goyal, T.; Saha, R. K. Modelling of pyrolysis of coal–biomass blends using thermogravimetric analysis. *Bioresour. Technol.* **2008**, *99* (17), 8022–8026.
- (17) Vuthaluru, H. B. Investigations into the pyrolytic behaviour of coal/biomass blends using thermogravimetric analysis. *Bioresour. Technol.* **2004**, *92* (2), 187–195.
- (18) Moghtaderi, B.; Meesri, C.; Wall, T. F. Pyrolytic characteristics of blended coal and woody biomass. *Fuel* **2004**, *83* (6), 745–750.
- (19) Collot, A. G.; Zhuo, Y.; Dugwell, D. R.; Kandiyoti, R. Co-pyrolysis and co-gasification of coal and biomass in bench-scale fixed-bed and fluidised bed reactors. *Fuel* **1999**, *78* (6), 667–679.
- (20) Krerkkaiwan, S.; Fushimi, C.; Tsutsumi, A.; Kuchonthara, P. Synergetic effect during co-pyrolysis/gasification of biomass and sub-bituminous coal. *Fuel Process. Technol.* **2013**, *115*, 11–18.
- (21) Sonobe, T.; Worasuwannarak, N.; Pipatmanomai, S. Synergies in co-pyrolysis of Thai lignite and corncob. *Fuel Process. Technol.* **2008**, *89* (12), 1371–1378.
- (22) Yang, X.; Yuan, C. Y.; Xu, J.; Zhang, W. J. Co-pyrolysis of Chinese lignite and biomass in a vacuum reactor. *Bioresour. Technol.* **2014**, *173*, 1–5.
- (23) Di Nola, G.; de Jong, W.; Spliethoff, H. TG–FTIR characterization of coal and biomass single fuels and blends under slow heating rate conditions: Partitioning of the fuel-bound nitrogen. *Fuel Process. Technol.* **2010**, *91* (1), 103–115.
- (24) Feroso, J.; Arias, B.; Moghtaderi, B.; Pevida, C.; Plaza, M. G.; Pis, J. J.; Rubiera, F. Effect of co-gasification of biomass and petroleum coke with coal on the production of gases. *Greenhouse Gases* **2012**, *2* (4), 304–313.
- (25) Zhang, L.; Xu, S. P.; Zhao, W.; Liu, S. Q. Co-pyrolysis of biomass and coal in a free fall reactor. *Fuel* **2007**, *86* (3), 353–359.
- (26) Wu, C. F.; Wang, Z. C.; Huang, J.; Williams, P. T. Pyrolysis/gasification of cellulose, hemicellulose and lignin for hydrogen production in the presence of various nickel-based catalysts. *Fuel* **2013**, *106*, 697–706.
- (27) Lanza, R.; Nogare, D. D.; Canu, P. Gas phase chemistry in cellulose fast pyrolysis. *Ind. Eng. Chem. Res.* **2009**, *48* (3), 1391–1399.
- (28) Solomon, P. R.; Serio, M. A.; Despande, G. V.; Kroo, E. Cross-linking reactions during coal conversion. *Energy Fuels* **1990**, *4* (1), 42–54.
- (29) Ibarra, J. V.; Moliner, R.; Gavilan, M. P. Functional-group dependence of cross-linking reactions during pyrolysis of coal. *Fuel* **1991**, *70* (3), 408–413.
- (30) Aznar, M. P.; Caballero, M. A.; Sancho, J. A.; Frances, E. Plastic waste elimination by co-gasification with coal and biomass in fluidized bed with air in pilot plant. *Fuel Process. Technol.* **2006**, *87* (5), 409–420.
- (31) Storm, C.; Rudiger, H.; Spliethoff, H.; Hein, K. R. G. Co-pyrolysis of coal/biomass and coal/sewage sludge mixtures. *J. Eng. Gas Turbines Power* **1999**, *121* (1), 55–63.
- (32) Hosoya, T.; Kawamoto, H.; Saka, S. Secondary reactions of lignin-derived primary tar components. *J. Anal. Appl. Pyrolysis* **2008**, *83* (1), 78–87.
- (33) Xin, S. Z.; Yang, H. P.; Chen, Y. Q.; Wang, X. H.; Chen, H. P. Assessment of pyrolysis polygeneration of biomass based on major components: Product characterization and elucidation of degradation pathways. *Fuel* **2013**, *113*, 266–273.
- (34) Wang, M. J.; Tian, J. L.; Roberts, D. G.; Chang, L. P.; Xie, K. C. Interactions between corncob and lignite during temperature-programmed co-pyrolysis. *Fuel* **2015**, *142*, 102–108.
- (35) Wang, J. F.; Yan, Q. X.; Zhao, J. T.; Wang, Z. Q.; Huang, J. J.; Gao, S. P.; Song, S. S.; Fang, Y. T. Fast co-pyrolysis of coal and biomass in a fluidized-bed reactor. *J. Therm. Anal. Calorim.* **2014**, *118* (3), 1663–1673.
- (36) Song, Y. Y.; Tahmasebi, A.; Yu, J. L. Co-pyrolysis of pine sawdust and lignite in a thermogravimetric analyzer and a fixed-bed reactor. *Bioresour. Technol.* **2014**, *174*, 204–211.
- (37) Quan, C.; Xu, S. P.; An, Y.; Liu, X. L. Co-pyrolysis of biomass and coal blend by TG and in a free fall reactor. *J. Therm. Anal. Calorim.* **2014**, *117* (2), 817–823.
- (38) Li, S. D.; Chen, X. L.; Liu, A. B.; Wang, L.; Yu, G. S. Study on co-pyrolysis characteristics of rice straw and Shenfu bituminous coal blends in a fixed bed reactor. *Bioresour. Technol.* **2014**, *155*, 252–257.
- (39) Yuan, S.; Dai, Z. H.; Zhou, Z. J.; Chen, X. L.; Yu, G. S.; Wang, F. C. Rapid co-pyrolysis of rice straw and a bituminous coal in a high-frequency furnace and gasification of the residual char. *Bioresour. Technol.* **2012**, *109*, 188–197.
- (40) Jones, J. M.; Kubacki, M.; Kubica, K.; Ross, A. B.; Williams, A. Devolatilisation characteristics of coal and biomass blends. *J. Anal. Appl. Pyrolysis* **2005**, *74* (1–2), 502–511.